

C.P. No. 233

(18,018)

A.R.C. Technical Report

C.P. No. 233

(18,018)

A.R.C. Technical Report



MINISTRY OF SUPPLY

AERONAUTICAL RESEARCH COUNCIL

CURRENT PAPERS

ROYAL AIR FORCE
RESEARCH ESTABLISHMENT
BEDFORD.

**A Technique for the Measurement
of Pressure Distribution on Oscillating
Aerofoils, with Results for a
Rectangular Wing of Aspect Ratio 3.3**

By

W. G. Molyneux, B.Sc. and F. Ruddlesden, A.M.I.E.I.

LONDON: HER MAJESTY'S STATIONERY OFFICE

1956

PRICE 3s. 6d. NET

U.D.C. No. 533.6.013.42:533.691:533.69.048.1

Technical Note No. Structures 164

June, 1955

ROYAL AIRCRAFT ESTABLISHMENT

A technique for the measurement of pressure distribution on oscillating aerofoils, with results for a rectangular wing of aspect ratio 3.3

by

W. G. Molyneux, B.Sc.
and
F. Ruddlesden, A.M.I.E.I.

SUMMARY

Details are given of a strain gauge pressure transducer that has been developed for measurements of pressure distribution on oscillating aerofoils in low speed wind tunnels. The transducer characteristics are shown to be well suited to oscillatory measurements, and in particular the transducer output can be measured directly on a sensitive galvanometer without the need for pre-amplification.

As an illustration of the use of the transducer, pressure measurements have been made in the R.A.E. 5 ft diameter open jet wind tunnel on a rectangular wing of aspect ratio 3.3 oscillating in modes of pitch and roll. Values for the aerodynamic derivatives have been obtained from the integrated pressure distributions, and are compared with those derived from overall force measurements and with theoretical values. The measured values are in close agreement but there are some discrepancies with theory that are thought to be due to a wind tunnel interference effect.

LIST OF CONTENTS

	<u>Page</u>	
1	Introduction	3
2	Required characteristics for a pressure transducer	3
3	Details of pressure transducer	4
3.1	Determination of transducer characteristics	4
3.11	Static characteristics	4
3.12	Dynamic characteristics	5
4	Pressure measurements on a rectangular wing of aspect ratio 3.3	6
4.1	Wind tunnel tests	6
4.2	Results	7
4.21	Pitch about the leading and trailing edges	7
4.22	Roll about the roll axis	7
4.3	Comparisons with theory and with results from overall force measurements on the wing	7
5	Conclusions	8
	Notation	9
	References	10

LIST OF TABLES

	<u>Table</u>
Forces and moments from integrated pressure distributions	I
Comparison of measured and theoretical derivative values	II

LIST OF ILLUSTRATIONS

	<u>Figure</u>
Details of strain gauge pressure transducer	1
Diagrammatic layout of pump	2
Variation of pump pressure with frequency	3
Square wave generator	4
Relay switch unit	5
Rectification by relay switch unit	6
Dynamic response characteristics of transducer	7
Locations of pressure transducers	8
Chordwise pressure distributions - wing pitch	9
Spanwise lift distribution - wing pitch	10
Spanwise distribution of pitching moment about wing leading edge - wing pitch	11
Spanwise distribution of rolling moment about wing root - wing pitch	12
Pressure, lift, pitch moment and roll moment distributions - wing roll	13
Spanwise variation of aerodynamic axis positions	14

1 Introduction

In theoretical investigations of aircraft flutter and oscillatory stability the greatest uncertainty lies in the values of the aerodynamic coefficients to be used. Coefficients derived theoretically^{1,2} are generally used but there is some evidence that these may differ considerably from measured values^{3,4}. There is an obvious need for experimental data to compare with theory, and with this object considerable effort is being devoted to aerodynamic force measurements on rigid aerofoils oscillating in simple modes^{3,4,5}. While these measurements are of value in providing a comparison with the overall forces predicted theoretically, they do not provide information on the distribution of force over the wing; nor can the techniques readily be adapted to enable force measurements to be made on flexible wings.

Both these difficulties can be overcome by measuring the pressure distribution over the oscillating aerofoil. However the problem here is mainly that of developing an instrument with suitable characteristics for oscillatory pressure measurements, and which is small enough to be buried within the aerofoil and simple enough to be produced in the comparatively large quantities required.

In what follows a pressure transducer that meets these requirements is described. The transducer is of the resistance strain gauge type and its output can be measured directly on a sensitive galvanometer without the need for pre-amplification. As an illustration of the use of the transducer, pressure measurements have been made in the R.A.E. 5 ft diameter wind tunnel on a rigid rectangular wing of aspect ratio 3.3 oscillating in modes of pitch about two axes and roll about the root. A total of twenty-seven transducers was used.

By integrating the measured pressure distributions the forces and moments on the wing have been determined, and the corresponding values of the oscillatory aerodynamic derivatives have been obtained. These derivatives are compared with those obtained by Guyett from overall force measurements on the wing, and generally the agreement is good. There are however some discrepancies between measured and theoretical values, but these are attributed to wind tunnel interference and the effect is being investigated separately.

2 Required characteristics for a pressure transducer

The following are considered to be the major desirable characteristics for a transducer to measure aerodynamic pressure on oscillating aerofoils

- (a) The transducer output should be linear with applied pressure.
- (b) The output should be insensitive to the inertia loads imposed under oscillatory conditions.
- (c) The output should be such that the minimum of subsidiary equipment is required to enable adequate detection of the signal.
- (d) There should be no lag between pressure and transducer response.
- (e) The transducer should be small enough to be buried within the aerofoil in the region of pressure measurement, thus avoiding a lag in response due to remoteness from the pressure source.
- (f) The resonant frequencies of all components should be well above the frequency range for pressure measurements.

(g) The design should permit large numbers to be produced with consistent characteristics.

The type of instrument that is developed to meet these requirements will depend on the conditions under which it is intended to operate. For example a more sensitive instrument will generally be necessary for low speed work than for high speeds, and a larger transducer may be permissible in the former case than in the latter. Furthermore, the frequency of excitation required to achieve a particular frequency parameter will generally increase in proportion to tunnel speed, and this in turn will influence the required resonance characteristics of the transducer.

3 Details of the pressure transducer

The transducer that is described here was developed for pressure measurements in a low speed tunnel (top speed 280 ft/sec) at frequencies within the range from 0 to 20 cycles per second. Measurements of pressures down to about 0.5 lb per square foot were required.

Preliminary investigations and experiments demonstrated that a transducer of the resistance strain gauge type offered the best possibility of satisfying the major requirements, and the transducer shown in Fig.1 was finally developed. The essential component of the transducer is a cylindrical unstretched rubber diaphragm to which is cemented a winding of resistance strain gauge wire. The diaphragm is cemented to a plastic core in which there are air passages to enable pressure from one source to be applied to the inside of the diaphragm, and an air space in the plastic cover enables pressure from another source to be applied to the outside. This arrangement enables the transducer to be buried within an aerofoil with one side communicating with one surface of the aerofoil and the other with the corresponding point on the opposite surface, thus measuring the pressure difference between the two surfaces.

The wire winding comprises two strain gauges each of $2\frac{1}{2}$ turns and about 250 ohms resistance, and these gauges are connected as two arms of a Wheatstone's bridge circuit. Application of pressure to either the inside or outside of the diaphragm produces a change in resistance of the gauges, and with voltage applied to the bridge this change of resistance is proportional to the current through a galvanometer placed across the bridge. To obtain a good detection of the signal a galvanometer of high sensitivity and low internal resistance is required. For the tests described here a galvanometer with a sensitivity of 98 mm/ μ A and an internal resistance of 152 ohms was used.

3.1 Determination of transducer characteristics

3.11 Static characteristics

Static calibrations of the transducer showed that the output was linear with applied pressure up to the point at which the diaphragm "cockled" and collapsed inwards. This occurred with an external pressure or internal suction applied to the diaphragm of about 60 lb per square foot, and determined the upper limit of operation of the transducer.

The sensitivity of the transducer increased linearly with applied voltage until the heat generated in the strain gauge windings began to affect the diaphragm. This occurred when the current through the windings was about 50 mA, but a current of about half this value, corresponding to 12.5 volts applied to the transducer bridge, is probably the safe upper limit for long term use. This determines the maximum sensitivity that can be obtained.

3.12 Dynamic characteristics

For dynamic calibrations a sinusoidal oscillating pressure was provided by the motor driven pump shown in Fig.2. The stroke of the pump was indicated by the deflection of a strain gauged cantilever strip attached to the plunger. A calibration of the variation of pump pressure with frequency showed that the transition from isothermal to adiabatic conditions within the pump followed the curve shown in Fig.3, the transition being virtually complete at frequencies greater than about 5 cycles per second. By using this curve the dynamic pressure at a particular frequency could be determined from a static measurement on a water tube manometer of the change of pressure with pump stroke.

The pump was connected by a rubber tube to one side of the transducer, and the other side of the transducer was open to atmosphere. Oscillation of the pump plunger pressurised the diaphragm and produced an oscillating output from the transducer bridge circuit.

To determine the phase lag between pressure application and transducer response it was necessary to obtain the components of the bridge output in phase and in quadrature with the motion of the pump plunger. The method used was based upon rectification at the pump frequency of the outputs from the transducer bridge and from the bridge on the cantilever indicating pump stroke, using the circuits shown in Figs. 4 and 5. A two segment commutator, one half at positive potential and the other negative, was fitted to the drive shaft of the pump motor, and from two pairs of brushes at 90° to each other two square wave output signals at 90° phase angle were obtained. Each output could be selected and fed to the energising coil of a relay switch unit which carried the bridge signal, thus reversing the signal for each half cycle of the commutator. The effect is seen in Fig.6. Suppose the bridge output is of amplitude S_0 and that switching occurs at phase angles $\psi, \psi + 180^\circ, \psi + 360^\circ$ etc. from one pair of brushes, and at $\psi + 90^\circ, \psi + 270^\circ$, etc. from the other pair. Then the mean direct current levels of the rectified signals due to switching are:-

$$\text{Mean level first pair} = - \int_{\psi}^{\psi+180^\circ} S_0 \sin \theta \, d\theta = - \frac{2 S_0}{\pi} \cos \psi$$

$$\text{Mean level second pair} = - \int_{\psi}^{\psi+270^\circ} S_0 \sin \theta \, d\theta = \frac{2 S_0}{\pi} \sin \psi .$$

$S_0 \cos \psi$ and $S_0 \sin \psi$ are the components at 90° of S_0 with a factor $\frac{2}{\pi}$ due to rectification, and these mean levels can be measured directly on the galvanometer. In this way the components of transducer response in phase and in quadrature with the pump stroke were obtained.

Using this arrangement the dynamic response characteristics of the transducer were determined, and are shown in Fig.7. It can be seen that the transducer response is linear with applied pressure (Fig.7(b)); there are no apparent resonances of transducer components within the frequency range from 0 to 40 cycles/sec (Fig.7(c)), and there is no measurable effect on transducer response of tube lengths between pump and transducer of up to 35 inches (Fig.7(d)).

For all these tests there was no measurable phase lag between pump stroke and transducer response, though a phase angle of about 1° could have been detected. This is particularly surprising where there is an appreciable tube length between pump and transducer, but the effect here will depend on the frequency of pressure fluctuation, and presumably at higher frequencies a measurable phase lag would be obtained. The characteristic is of value for low frequency pressure measurements on thin aerofoil sections where the transducer cannot be buried within the contour; the transducer need not be in the immediate vicinity, but can be connected to the pressure source by a tube.

In a further test to investigate the effects of inertia loads on transducer response a sealed transducer was attached to the pump plunger and oscillated with an amplitude of $\pm \frac{1}{8}$ " at frequencies up to 40 cycles/sec. No effect of inertia could be detected.

It is apparent therefore that for pressure measurements in a low speed wind tunnel the transducer has all the desirable qualities listed in section 2, the only factor remaining in doubt being reliability under test conditions. This was put to test in pressure measurements on a rectangular unswept wing.

4 Pressure measurements on a rectangular wing of aspect ratio 3.3

The wing used was not specially designed for pressure measurements but had previously been used in tests to measure overall aerodynamic forces under oscillatory conditions. It was thought that these overall force measurements would provide a useful check on the forces obtained by integrating the measured pressure distribution. Unfortunately the wing design did not allow transducers to be installed further forward than 0.8 inches from the leading edge.

The locations of the transducers were as shown in Fig.8. There were three major sections for pressure measurements, at about 0.48 span, 0.84 span and 0.96 span outboard from the root reflector plate, and single transducers were located between these sections along a spanwise axis at 0.325 span aft of the leading edge. A total of 27 transducers was used and their sensitivities were all within $\pm 5\%$ of the mean value. The power supply to the transducer bridges was 10 volts D.C. and the connecting circuit enabled the output from each bridge to be selected individually.

The wing was supported vertically by cross spring bearings at the root attached to a heavy rigid frame. The locations of these bearings could be varied so that wing freedoms of pitch about the leading edge, pitch about the trailing edge or roll could be provided. The wing projected through a flat topped table with a sufficient gap around the wing to allow for wing oscillations. This gap was overlapped by the reflector plate attached at the root of the wing and oscillating with it. The gap between plate and table top was about 0.2 inches.

4.1 Wind tunnel tests

The tests were made in the R.A.E. 5 ft diameter open jet wind tunnel. The wing was mounted in the centre plane of the tunnel with the centre line of the table top some 6 inches above the edge of the jet boundary, and was excited through a rod at about 0.7 span. The rod was driven sinusoidally by a rider on a rotating swashplate, and the shaft of the motor driving the swashplate also carried the commutator required for bridge output rectification (section 3.22). Displacement of the wing was indicated by the bending of a cantilever strip between wing and supporting frame, strain gauges at the root of the cantilever being connected in a bridge circuit.

The wing was oscillated at a frequency of 6.5 cycles/second, this being the highest frequency at which the motor could be run. For the modes of pitch about the leading and trailing edges pressure measurements were made at a fixed tunnel speed of 200 ft/sec (frequency parameter 0.33) with incidence oscillating through ± 2.2 degrees, while for the roll mode the tunnel speed was 240 ft/sec (frequency parameter 0.275) and the roll angle ± 1.02 degrees. A higher speed was used in the latter case to provide a larger transducer response.

The test procedure adopted was to maintain tunnel speed, wing amplitude and frequency of oscillation constant, measure the rectified components of the output from the amplitude bridge, and select each transducer bridge in turn and measure its output components. These measurements could be made in less than one hour, and the same procedure was followed for each of the three modes of oscillation of the wing.

4.2 Results

From the above measurements the components of pressure at each measuring point in phase and in quadrature with the displacement of the wing were determined. The chordwise pressure distributions for pitching about the leading and trailing edges are shown in Fig.9 and those for wing roll in Fig.13.

4.21 Pitch about the leading and trailing edges

It can be seen that the in phase pressure distributions for both modes of oscillation are similar, a significant feature being that the pressure towards the tip becomes negative over the rear part of the wing. The in quadrature components differ markedly due to the pressure contribution arising from normal velocity of the wing. To enable integration of these pressure distributions the curves have been extended arbitrarily to the wing leading edge, and to enable the forces on the wing to be determined the spanwise curves through the points corresponding to the section integrals have been extended arbitrarily to the wing root. The spanwise distributions of the lift, pitching moment about the wing leading edge and rolling moment about the root are shown in Figs. 10-12, and the aerodynamic axis and centre of pressure positions for the two modes of oscillation are shown in Fig.14. The values for the forces and moments on the wing, expressed in terms of the oscillatory aerodynamic derivatives, are given in Table I, and the corresponding derivative values in Table II.

4.22 Roll about the roll axis

For this mode of oscillation pressure components in phase with the motion were negligibly small and only quadrature components could be detected. The chordwise pressure distribution and the spanwise distribution of lift, pitching moment and rolling moment about the roll axis are shown in Fig.13, and the aerodynamic axis and centre of pressure positions are shown in Fig.14. The derived forces and moments on the wing are given in Table I and the corresponding derivative values are given in Table II.

4.3 Comparisons with theory and with results from overall force measurements on the wing

The chordwise pressure distributions for the wing pitch modes are compared with the distributions predicted by two dimensional theory in Fig.9. As expected, the further inboard the section at which pressure measurements were made the more closely does the distribution approximate to the theoretical distribution. However, there are significant differences between the measured and theoretical in phase pressure

distribution near the wing trailing edge. In general the curves of measured pressure distribution are concave over this part of the wing whereas the theoretical curve is convex; furthermore, the measurements show a region of negative pressure towards the tip. Effects of this sort may offer an explanation for some of the marked differences that are obtained between measured and theoretical values of control surface derivatives^{3,4}.

The derivative values derived from the pressure measurements are compared in Table II with those obtained by Guyett (unpublished) from overall force measurements on the wing. Also included in the table are some theoretical derivatives obtained from the results of Lawrence and Gerber² for wings of low aspect ratio. It can be seen that generally the derivatives obtained by the two methods of measurement are in quite close agreement, which demonstrates the reliability of the pressure measuring technique. There are, however, some quite large discrepancies between the measured derivatives and theoretical values.

Some further measurements by Guyett⁶ of pitching moment derivatives on full span wings mounted in the centre of the tunnel show close agreement with theory, and it is therefore concluded that the discrepancy that obtains here is due to a wind tunnel error arising from mounting so large a wing close to the jet boundary. A theoretical explanation for the discrepancy has not yet been found, but further experimental work is in progress to establish its source.

5 Conclusions

The resistance strain gauge pressure transducer described here is shown to be well suited to oscillatory pressure measurements in low speed wind tunnels.

Transducers have been used for measurements in the R.A.E. 5 ft diameter open jet wind tunnel on a rectangular unswept wing of aspect ratio 3.3 oscillating in modes of wing pitch and roll. The oscillatory aerodynamic derivatives obtained from the integrated pressure distributions are in close agreement with those obtained from overall force measurements on the wing, but there are some discrepancies with theoretical values. These discrepancies are attributed to a wind tunnel error that is being investigated separately.

NOTATION

- s = Wing length, reflector plate to tip (32.8 ins)
- c = Wing chord (20 ins)
- S = Wing area (4.56 sq ft)
- A = aspect ratio $\frac{2s}{c}$ (3.28)
- ℓ = length, roll axis to wing tip (37.3 ins)
- V = Wind speed
- ρ = air density
- ω = frequency of oscillation of the wing
- ν = frequency parameter $\frac{\omega c}{V}$
- $\left. \begin{matrix} L_{\dot{z}} \\ L_z \end{matrix} \right\}$ = Non dimensional oscillatory derivative for lift $\left\{ \begin{matrix} \text{damping} \\ \text{stiffness} \end{matrix} \right\}$
at wing leading edge due to wing translation.
- $\left. \begin{matrix} L_{\dot{\alpha}} \\ L_{\alpha} \end{matrix} \right\}$ = Non dimensional oscillatory derivative for lift $\left\{ \begin{matrix} \text{damping} \\ \text{stiffness} \end{matrix} \right\}$
at wing leading edge due to pitch about leading edge.
- $\left. \begin{matrix} M_{\dot{z}} \\ M_z \end{matrix} \right\}$ = Non dimensional oscillatory derivative for pitching moment
 $\left\{ \begin{matrix} \text{damping} \\ \text{stiffness} \end{matrix} \right\}$ about wing leading edge due to wing translation.
- $\left. \begin{matrix} M_{\dot{\alpha}} \\ M_{\alpha} \end{matrix} \right\}$ = Non dimensional oscillatory derivative for pitching moment
 $\left\{ \begin{matrix} \text{damping} \\ \text{stiffness} \end{matrix} \right\}$ about wing leading edge due to pitch about
leading edge.
- $\left. \begin{matrix} N_{\dot{z}} \\ N_z \end{matrix} \right\}$ = Non dimensional oscillatory derivative for rolling moment
 $\left\{ \begin{matrix} \text{damping} \\ \text{stiffness} \end{matrix} \right\}$ about wing root due to wing translation.
- $\left. \begin{matrix} N_{\dot{\alpha}} \\ N_{\alpha} \end{matrix} \right\}$ = Non dimensional oscillatory derivative for rolling moment
 $\left\{ \begin{matrix} \text{damping} \\ \text{stiffness} \end{matrix} \right\}$ about wing root due to wing pitch about
leading edge.
- $\left. \begin{matrix} L_{\dot{\phi}} \\ L_{\phi} \end{matrix} \right\}$ = Non dimensional oscillatory derivative for lift $\left\{ \begin{matrix} \text{damping} \\ \text{stiffness} \end{matrix} \right\}$
at wing leading edge due to roll about roll axis.
- $\left. \begin{matrix} M_{\dot{\phi}} \\ M_{\phi} \end{matrix} \right\}$ = Non dimensional oscillatory derivative for pitching moment
 $\left\{ \begin{matrix} \text{damping} \\ \text{stiffness} \end{matrix} \right\}$ about wing leading edge due to roll about roll
axis.
- $\left. \begin{matrix} N_{\dot{\phi}} \\ N_{\phi} \end{matrix} \right\}$ = Non dimensional oscillatory derivative for rolling moment
 $\left\{ \begin{matrix} \text{damping} \\ \text{stiffness} \end{matrix} \right\}$ about roll axis edge due to roll about roll axis.

REFERENCES

- | <u>No.</u> | <u>Author</u> | <u>Title etc</u> |
|------------|------------------------------------|---|
| 1 | I.T. Mirhinnick | Subsonic aerodynamic derivatives for wings and control surfaces.
R.A.E. Report Structures 87. July 1950.
ARC 14,228 O.956 |
| 2 | H.R. Lawrence and
E.H. Gerber | The aerodynamic forces on low aspect ratio wings oscillating in incompressible flow.
Journal Aero Sciences Vo.19, No.11, P.769.
Nov. |
| 3 | K.C. Wight | Measurement of two dimensional derivatives on a wing aileron tab system.
ARC 15,292 O.1017. Oct. 1952. |
| 4 | W.G. Molyneux and
F. Ruddlesden | Derivative measurements and flutter tests on a rectangular wing with a full span aileron.
R.A.E. Report Structures 172. Feb. 1955.
ARC 17,751 |
| 5 | P.R. Guyett and
D.E.G. Poulter | Measurements of pitching moment derivatives for a series of rectangular wings at low wind speeds.
R.A.E. Report Structures 185.
ARC 18,012. June, 1955. |

TABLE I

Forces and Moments from Integrated Pressure Distributions

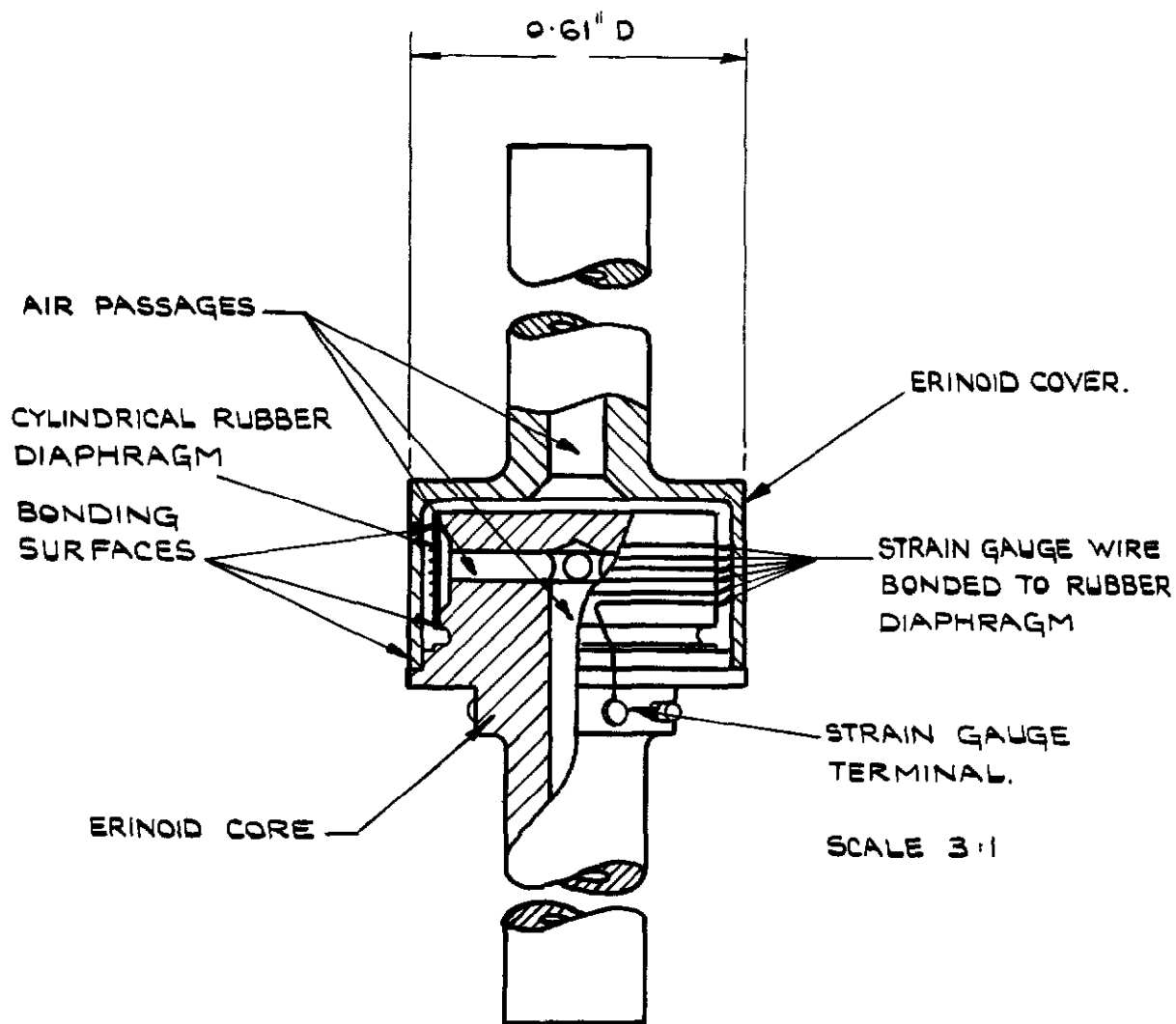
Pitch about leading edge			Pitch about trailing edge			Roll about roll axis		
Lift Force	In phase	22.3 lb	Lift force	In phase	25.8 lb	Lift force	In phase	-
$\rho V^2 S \alpha (L_\alpha + i\nu L_\alpha^*)$	In quad:	11.2 lb	$\rho V^2 S \alpha \{ (L_x - L_z) + i\nu (L_\alpha^* - L_z^*) \}$	In quad:	2.9 lb	$\rho V^2 S \phi (L_\phi + i\nu L_\phi^*)$	In quad:	3.6 lb
Nose up pitch moment about leading edge.	In phase	-6.9 lb ft	Nose up pitch moment about leading edge.	In phase	-8.4 lb ft	Nose up pitch moment about leading edge.	In phase	-
$\rho V^2 S c \alpha (M_\alpha + i\nu M_\alpha^*)$	In quad:	-7.9 lb ft	$\rho V^2 S c \alpha \{ (M_\alpha - M_z) + i\nu (M_\alpha^* - M_z^*) \}$	In quad:	-4.6 lb ft	$\rho V^2 S c \phi (M_\phi + i\nu M_\phi^*)$	In quad:	-1.1 lb ft
Roll moment about wing root.	In phase	27.2 lb ft	Roll moment about wing root.	In phase	30.2 lb ft	Roll moment about roll axis.	In phase	-
$\frac{1}{2} \rho V^2 S s \alpha (N_\alpha + i\nu N_\alpha^*)$	In quad:	14.1 lb ft	$\frac{1}{2} \rho V^2 S s \alpha \{ (N_\alpha - N_z) + i\nu (N_\alpha^* - N_z^*) \}$	In quad:	3.9 lb ft	$\frac{1}{2} \rho V^2 S s \phi (N_\phi + i\nu N_\phi^*)$	In quad:	6.7 lb ft

111

TABLE II

Comparison of measured and theoretical
derivative values

Frequency Parameter	Derivative	Measured Derivative Value		Theoretical Value Lawrence and Gerber ²
		Pressure Integration	Overall force measurement	
0.33	L_z	-0.20	-0.10	0.44
"	L_z	1.50	1.53	1.57
"	L_α	1.35	1.40	1.58
"	L_α	2.05	1.80	1.37
"	M_z	0.05	0.02	0.01
"	M_z	-0.36	-0.38	-0.41
"	M_α	-0.25	-0.27	-0.37
"	M_α	-0.86	-0.80	-0.69
"	N_z	-0.13	-0.20	
"	N_z	1.34	1.50	
"	N_α	1.20	1.20	
"	N_α	1.86	1.80	
0.275	L_ϕ	1.15	1.30	
"	M_ϕ	-0.21	-0.25	
"	N_ϕ	1.30	1.50	



DIAPHRAGM - 0.5" DIA. X 0.010" PAULS COLOTOMY TUBING.
 ADHESIVE - ACETONE BASED "TIGHTBOND"
 GAUGE WIRE - 0.001" DIA. NICHROME, 2075 OHMS/YD.

FIG. I. DETAILS OF STRAIN GAUGE PRESSURE TRANSDUCER.

FIG.2&3.

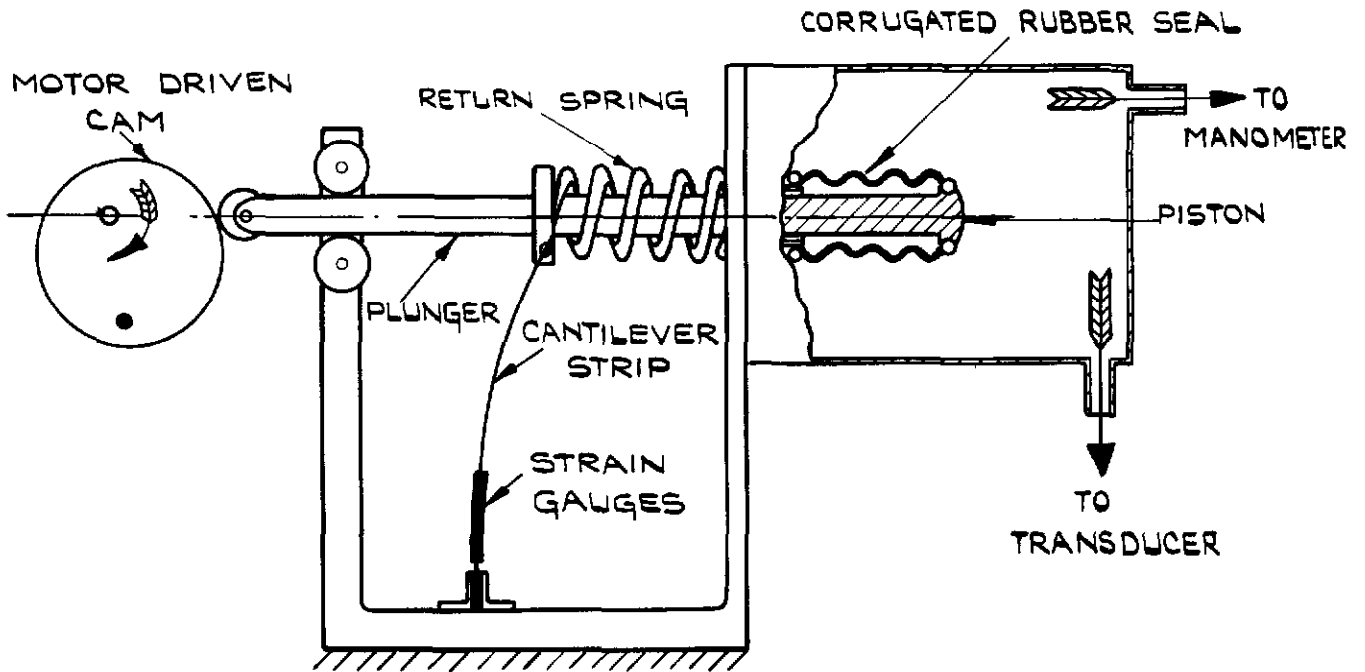


FIG.2. DIAGRAMMATIC LAYOUT OF PUMP.

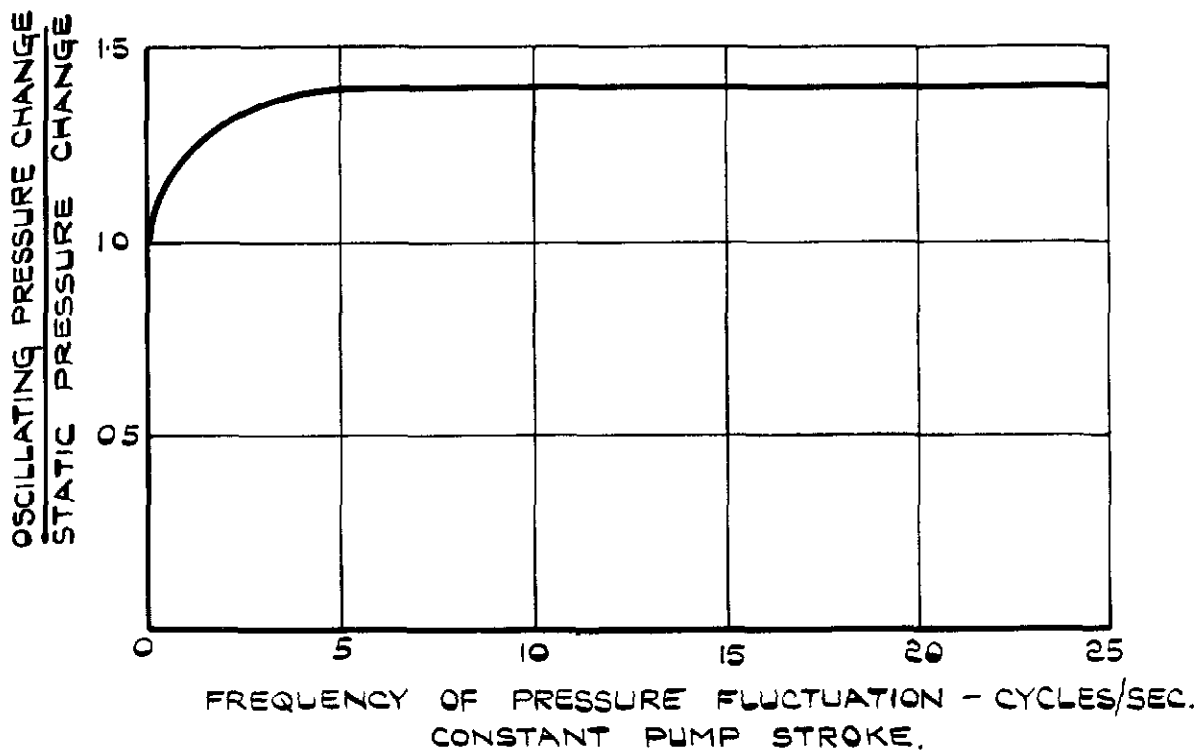


FIG.3. VARIATION OF PUMP PRESSURE WITH FREQUENCY.

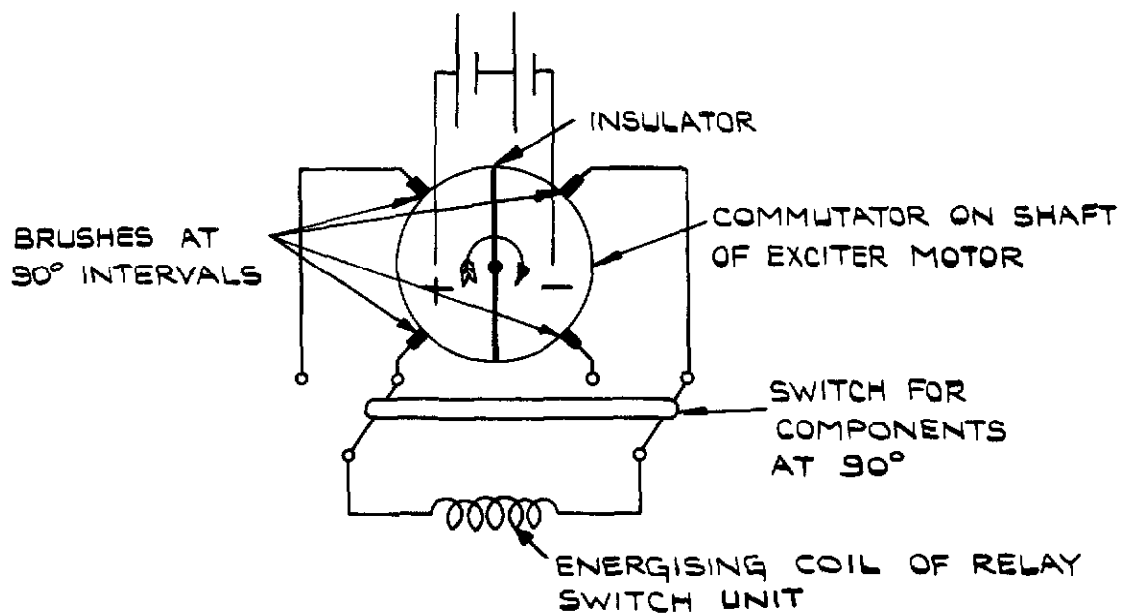


FIG. 4. SQUARE WAVE GENERATOR.

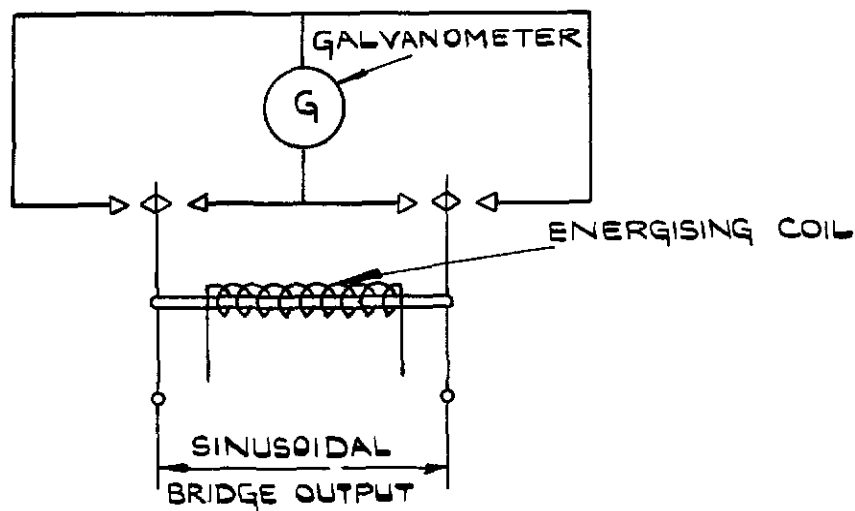


FIG . 5. RELAY SWITCH UNIT.

FIG. 6.

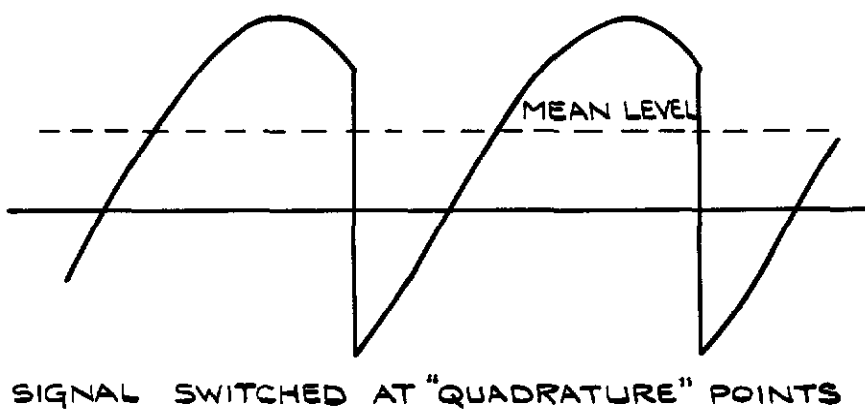
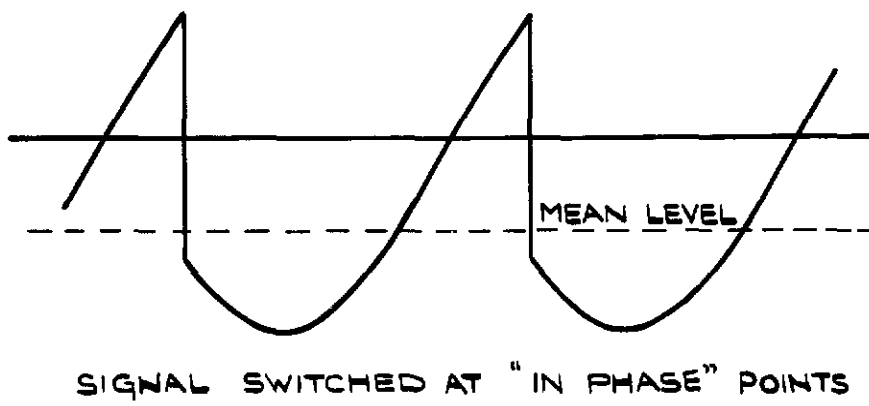
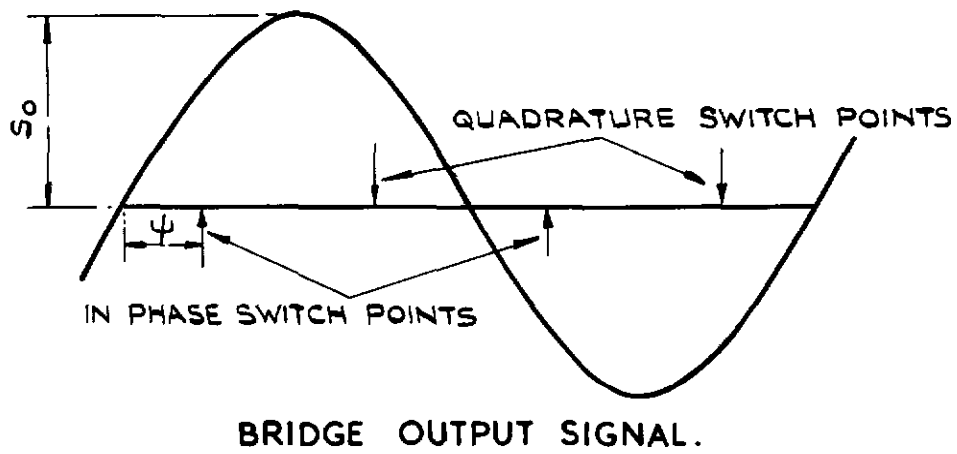
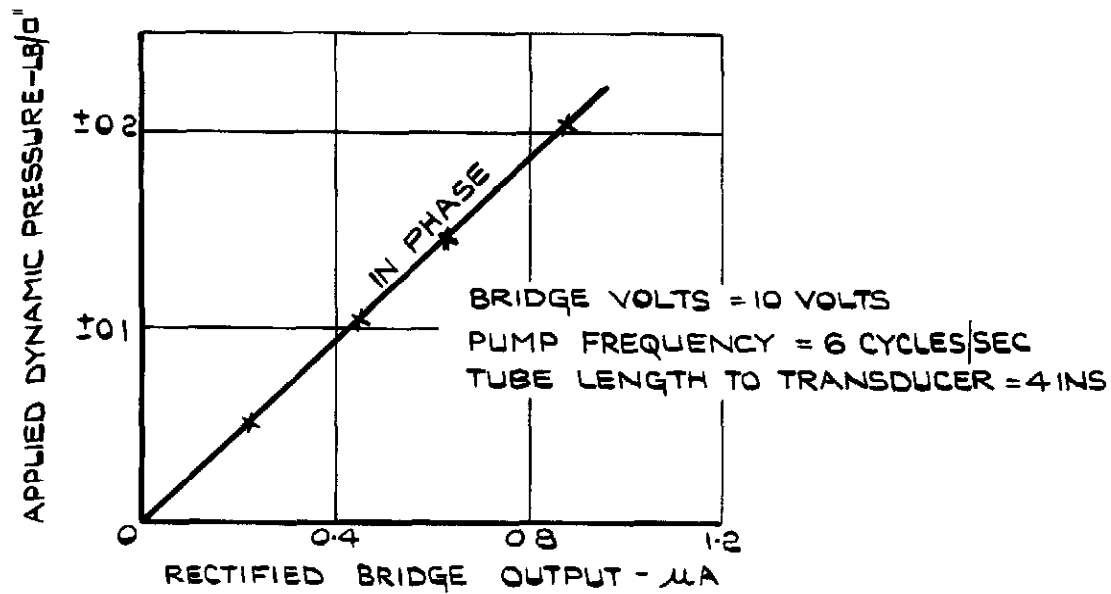
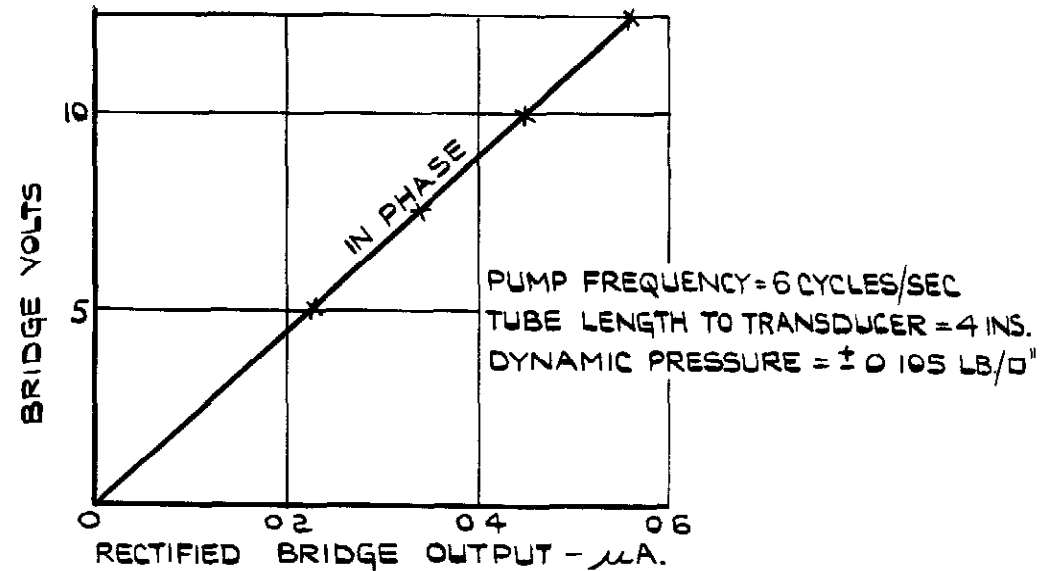


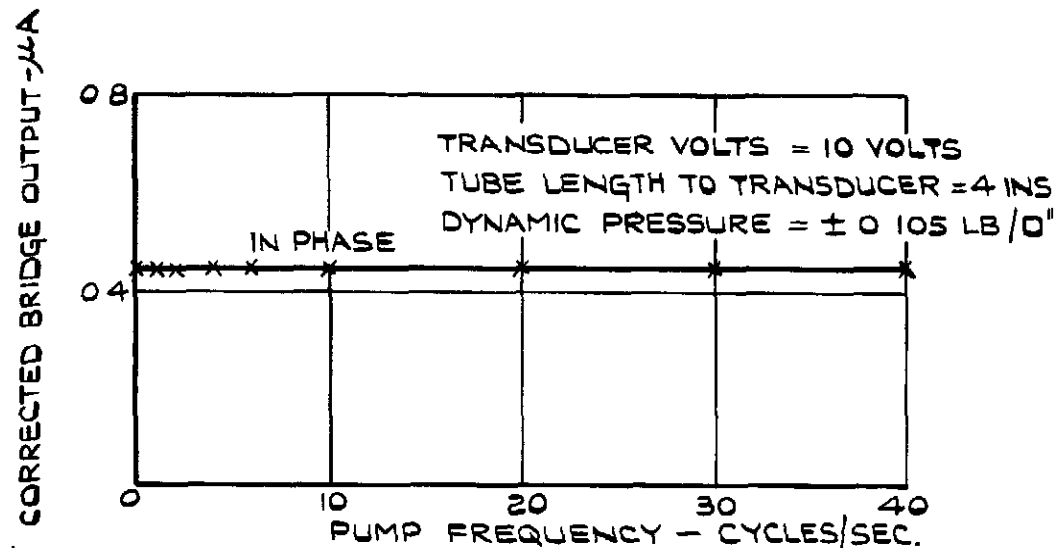
FIG.6. RECTIFICATION BY RELAY SWITCH UNIT.



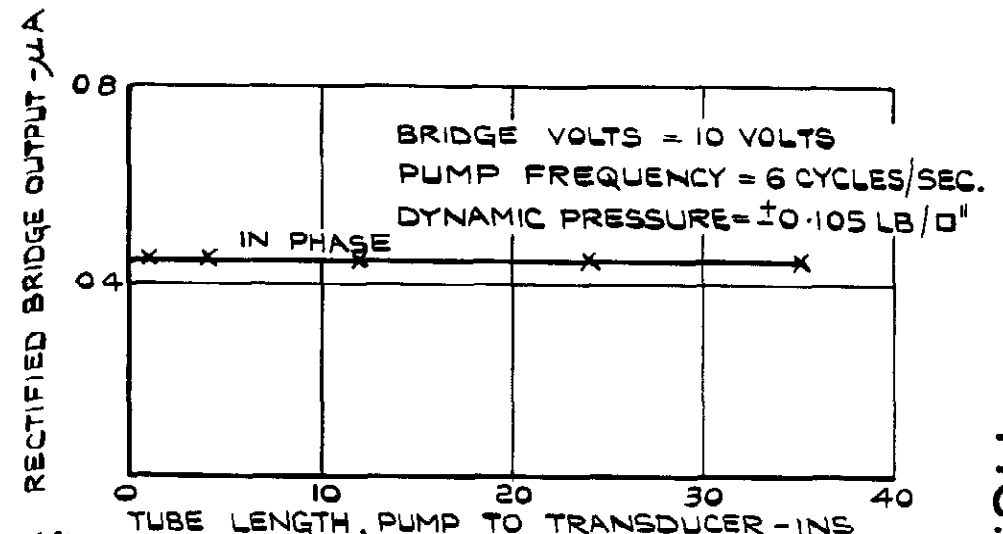
(a) LINEARITY OF TRANSDUCER RESPONSE TO APPLIED PRESSURE.



(b) LINEARITY OF TRANSDUCER OUTPUT WITH APPLIED VOLTAGE.



(c) VARIATION OF TRANSDUCER RESPONSE WITH FREQUENCY.



(d) VARIATION OF TRANSDUCER RESPONSE WITH TUBE LENGTH TO PUMP.

FIG. 7. (a - d) DYNAMIC RESPONSE CHARACTERISTICS OF TRANSDUCER.

FIG. 8.

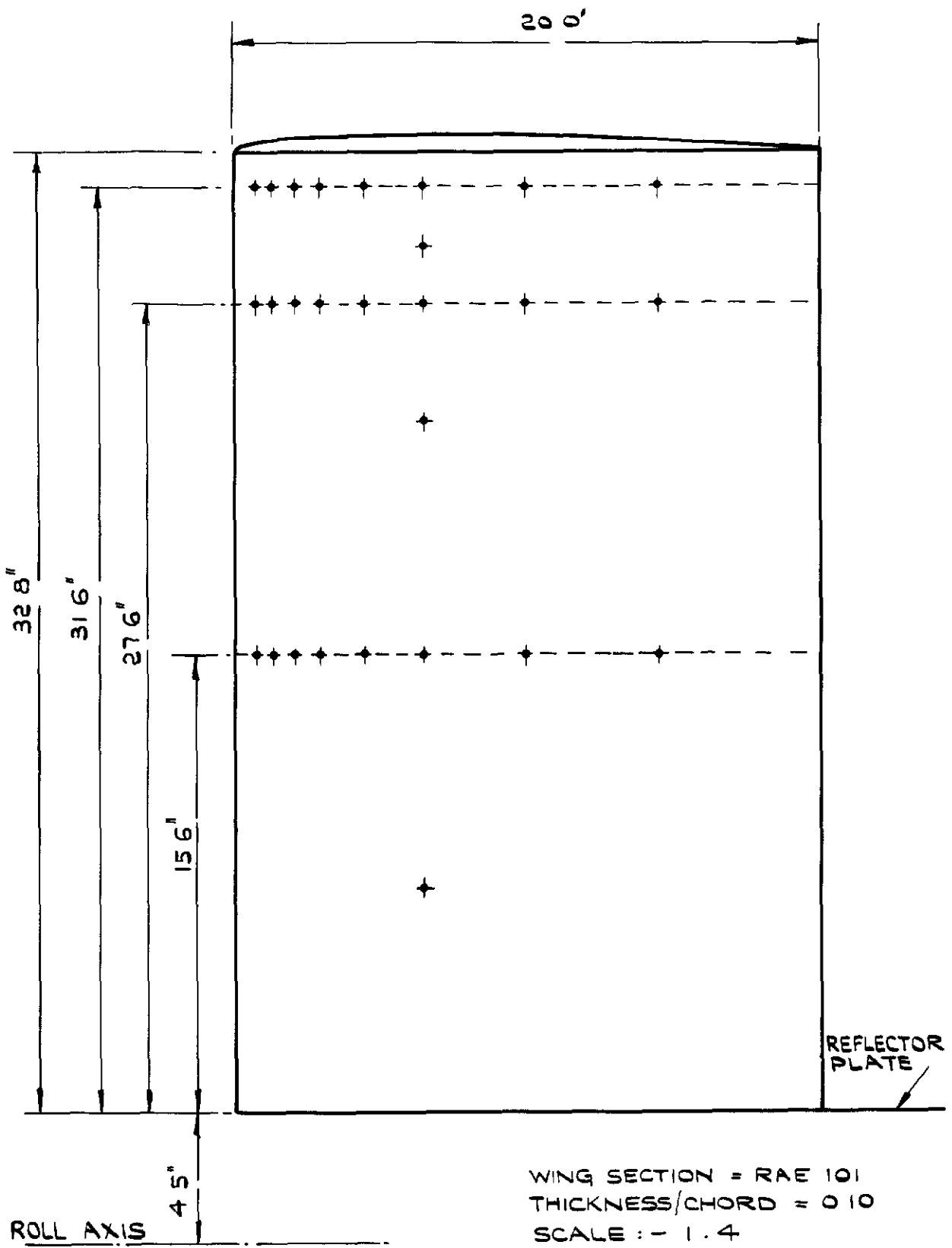
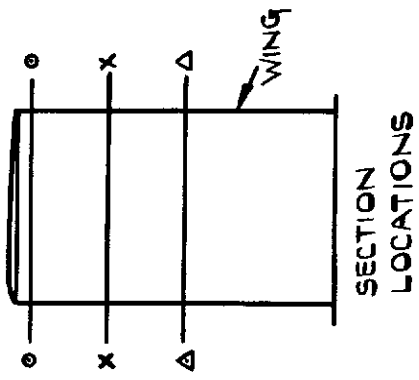
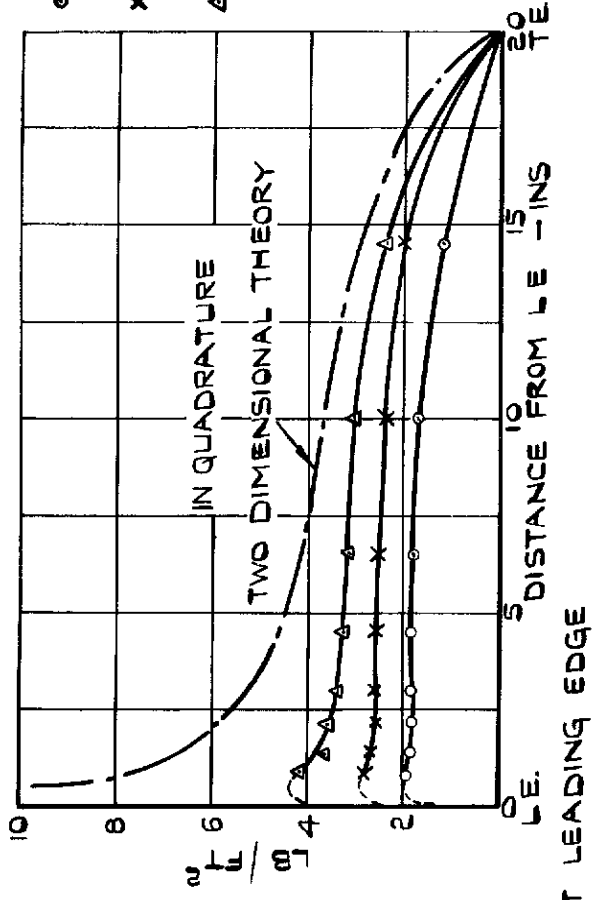
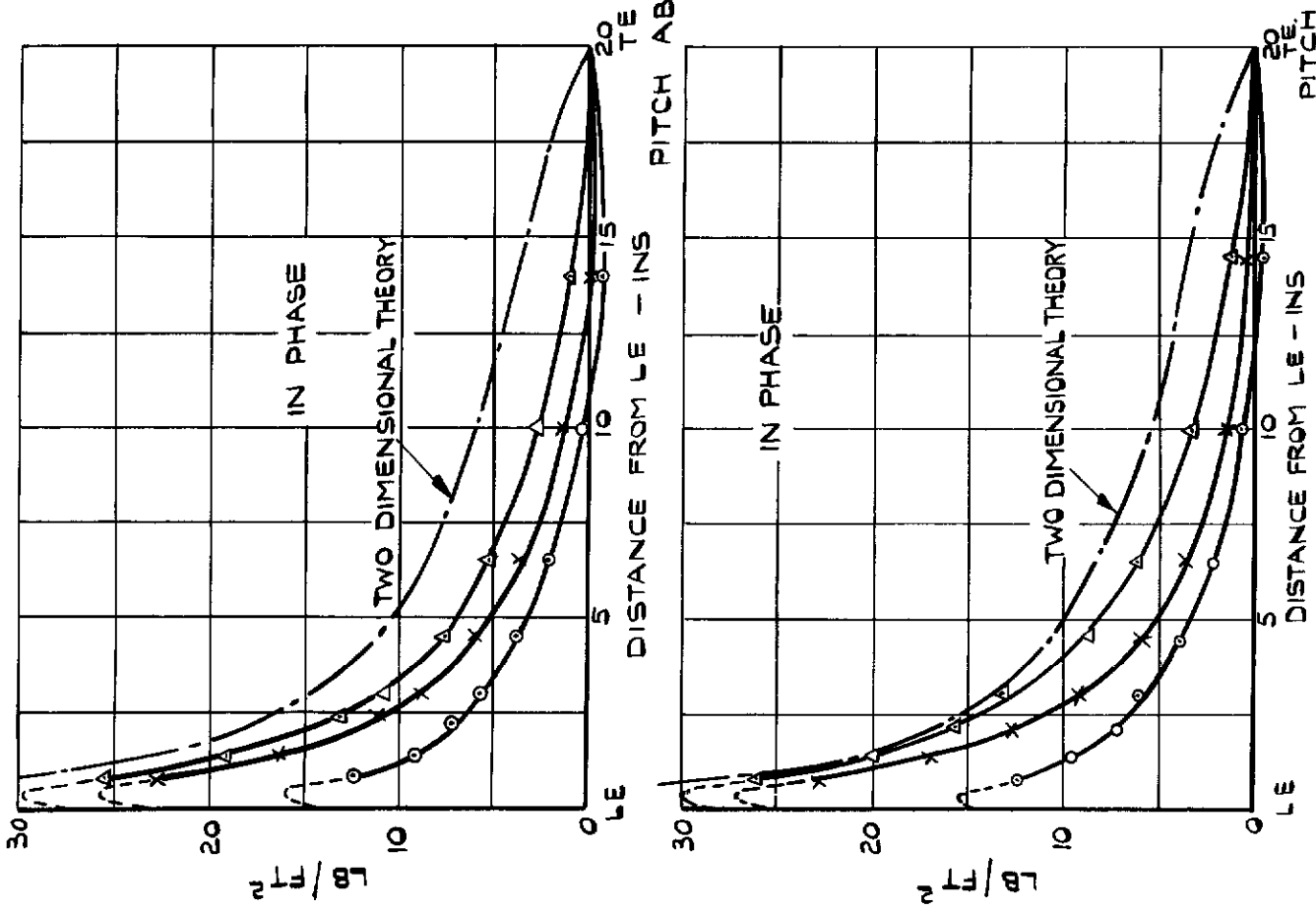


FIG. 8. LOCATIONS OF PRESSURE TRANSDUCERS.



WINDSPEED = 200 FT/SEC
 INCIDENCE = ±2.2 DEGREES
 FREQUENCY = 6.30 CYCLES/SEC

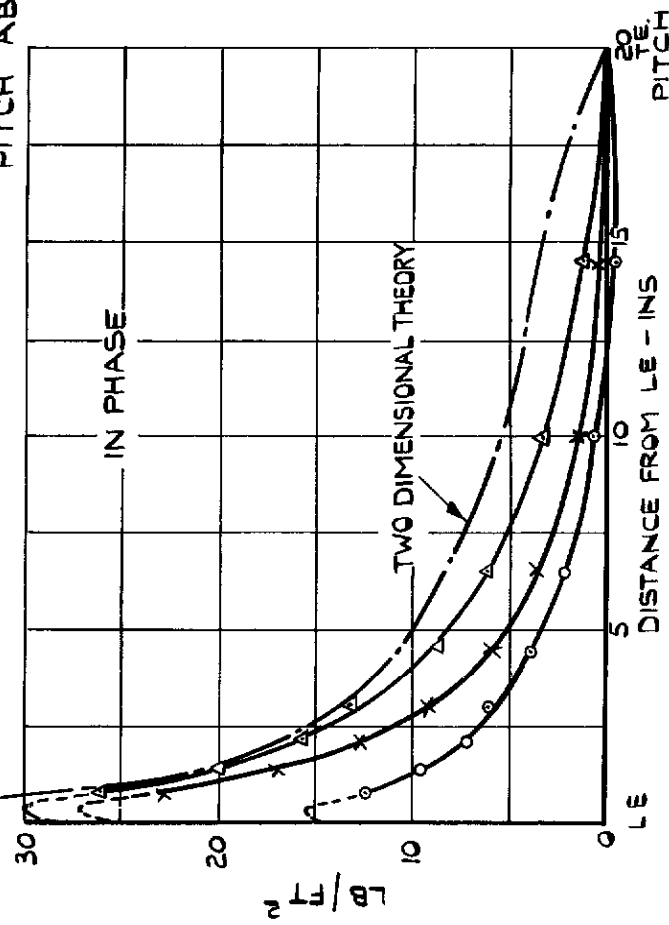


FIG. 9. CHORDWISE PRESSURE DISTRIBUTION - WING PITCH.

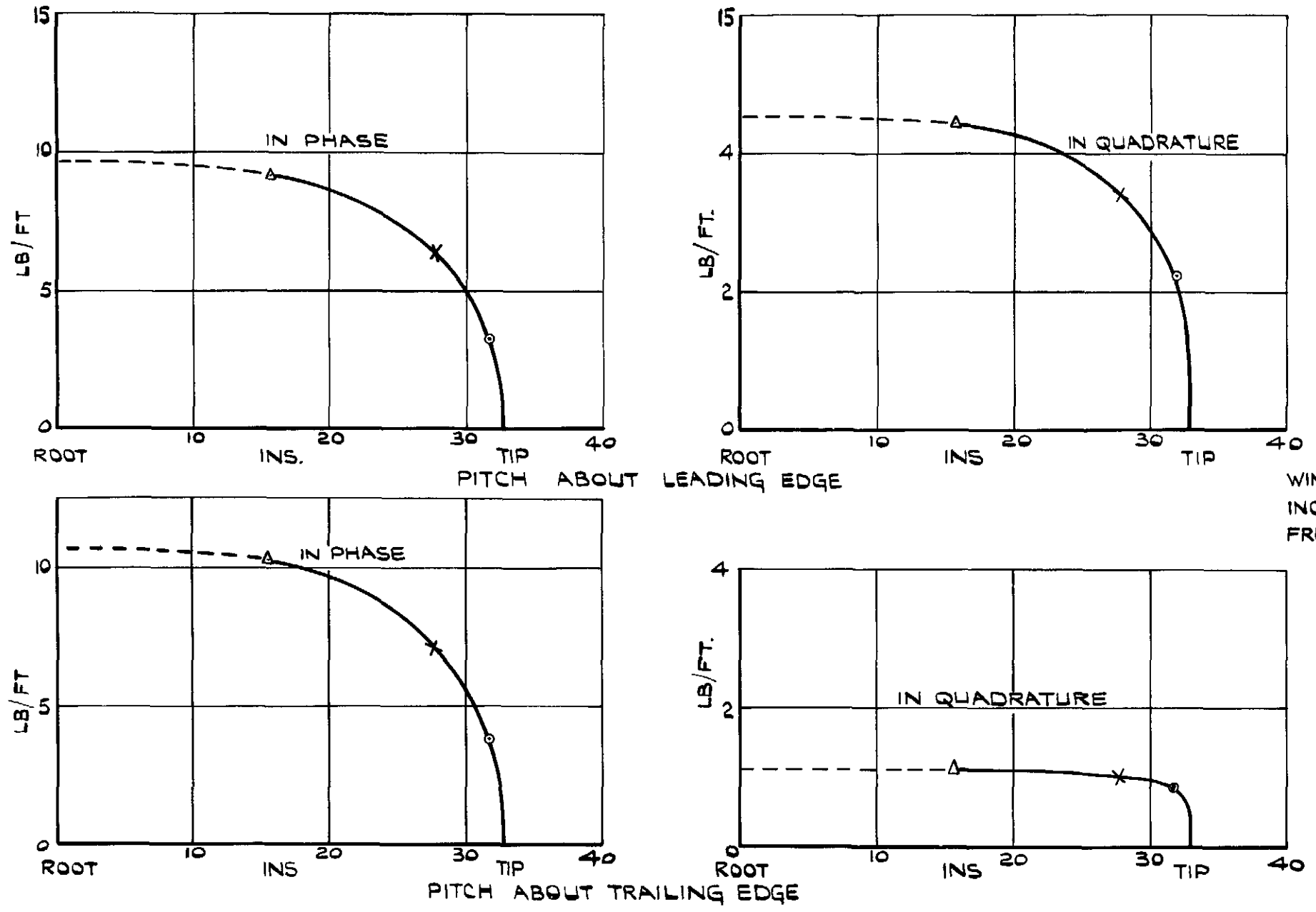
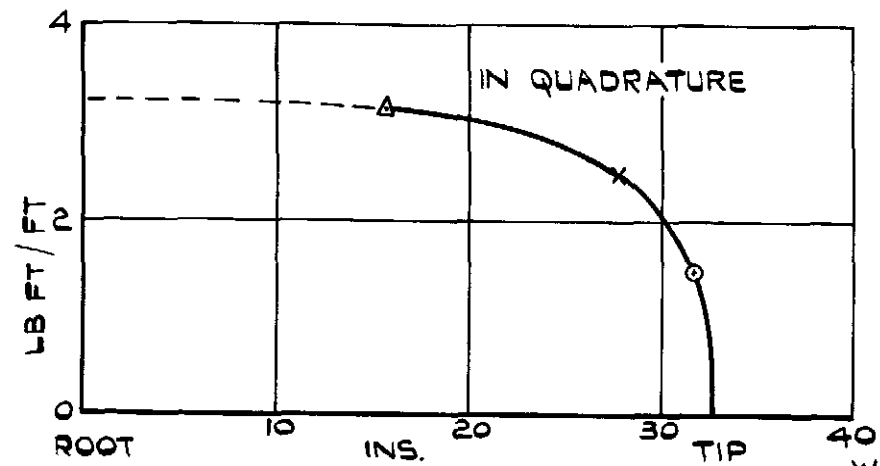
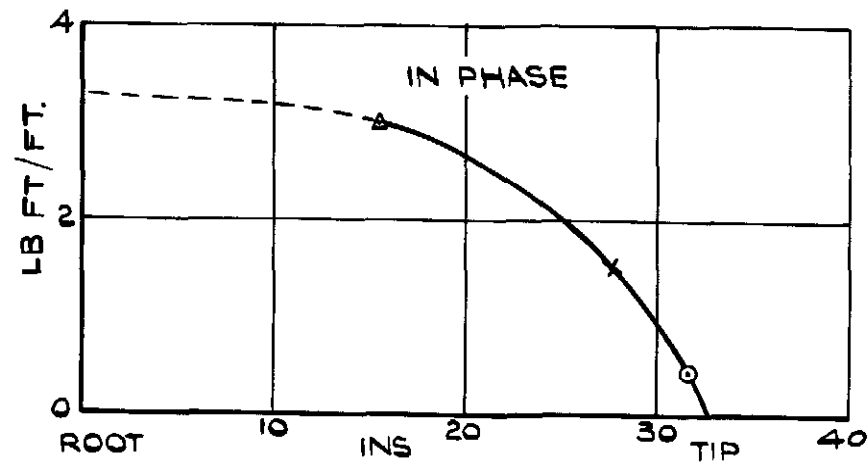


FIG. 10. SPANWISE LIFT DISTRIBUTION - WING PITCH.



WINDSPEED = 200 FT/SEC
 INCIDENCE = ±22 DEGREES
 FREQUENCY = 6.30 CYCLES/SEC

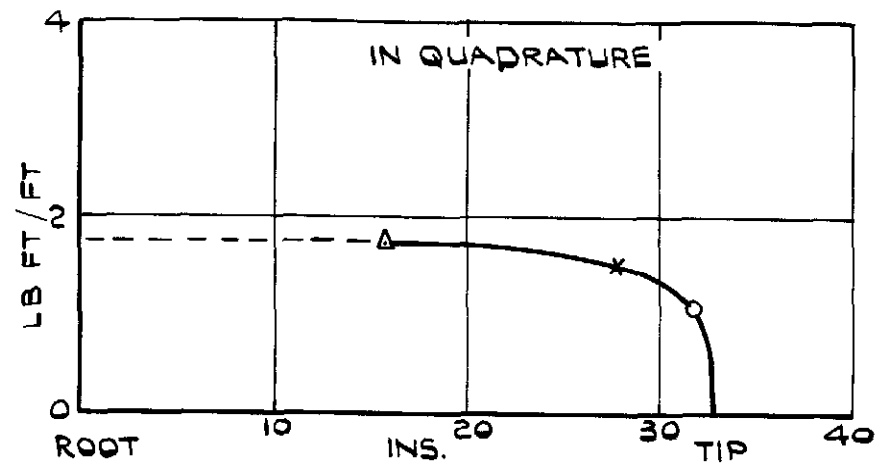
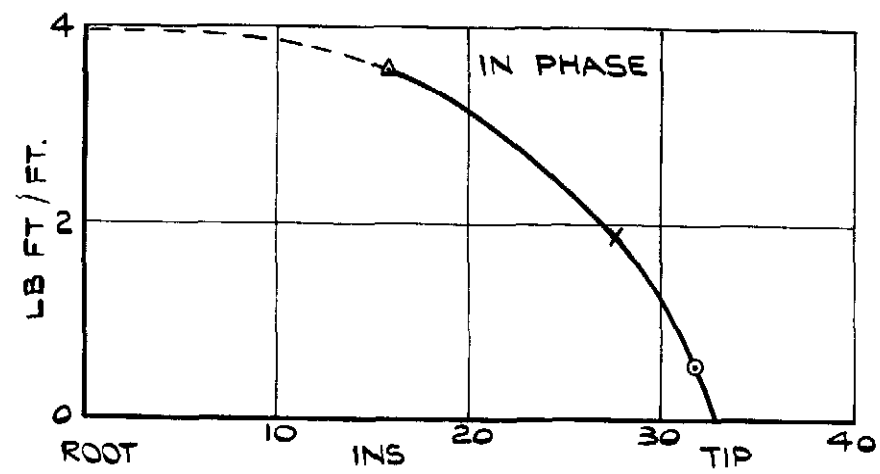
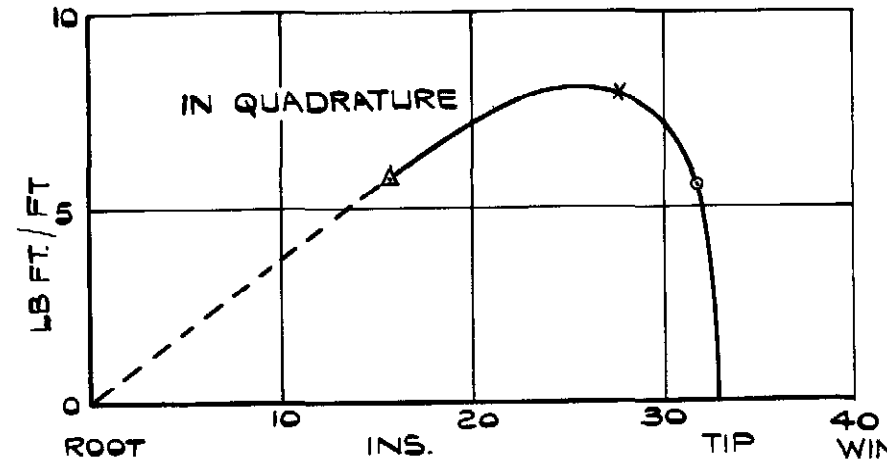
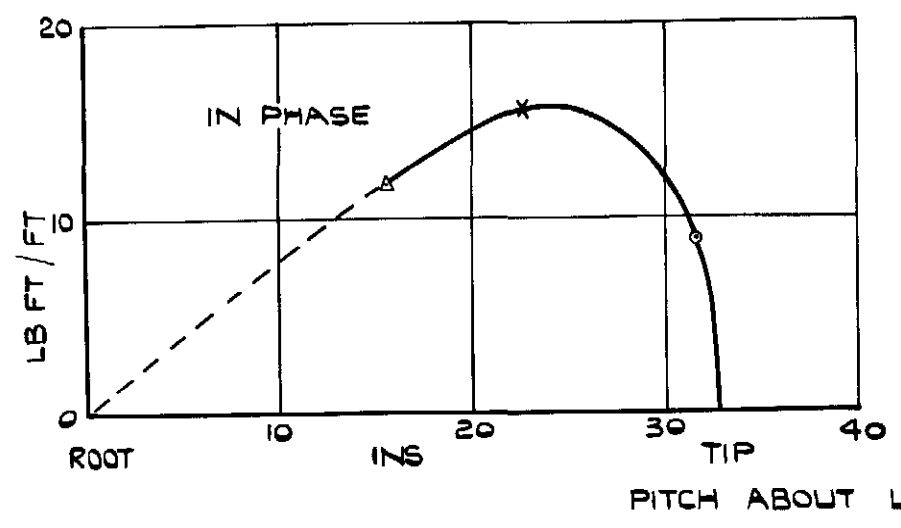


FIG. II. SPANWISE DISTRIBUTION OF PITCHING MOMENT ABOUT WING LEADING EDGE - WING PITCH.

FIG. II.



WINDSPEED = 200 FT/SEC
INCIDENCE = ±22 DEGREES
FREQUENCY = 630 CYCLES/SEC

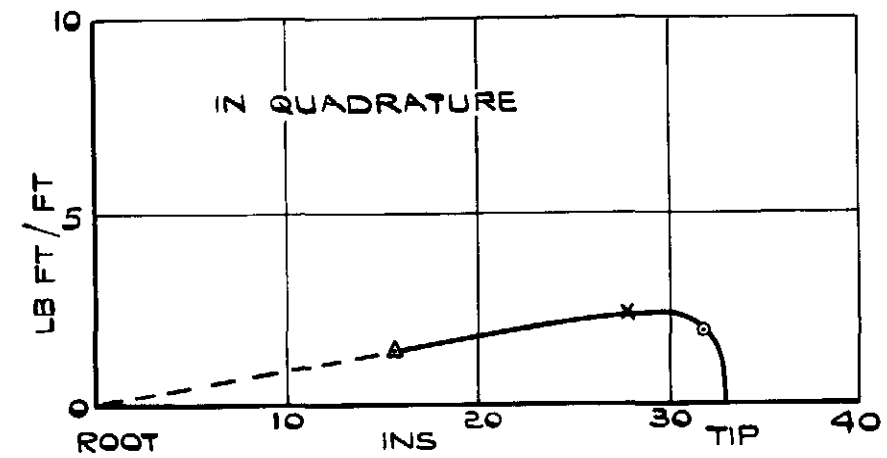
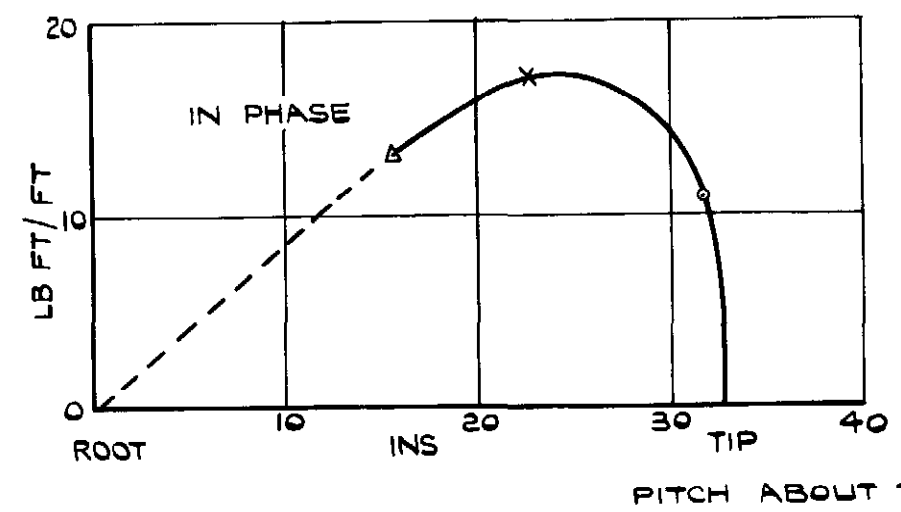
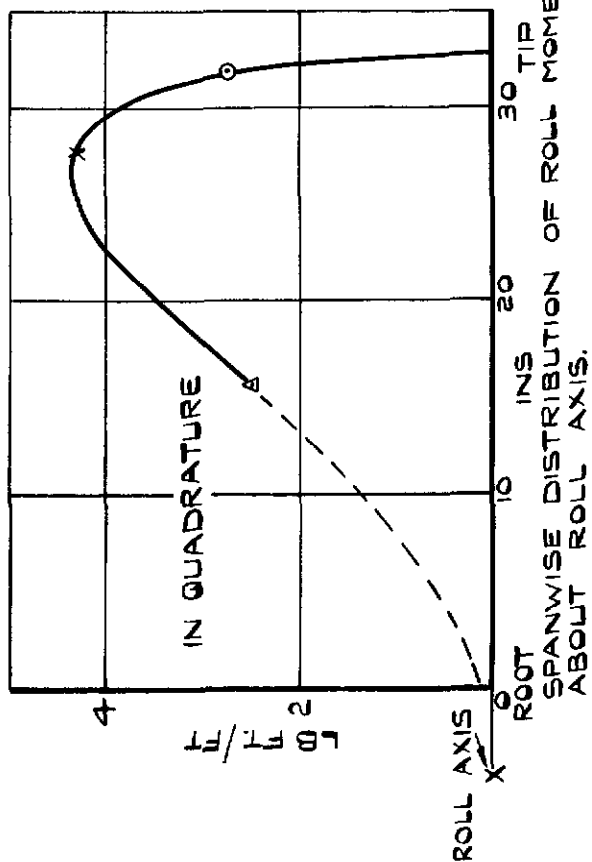
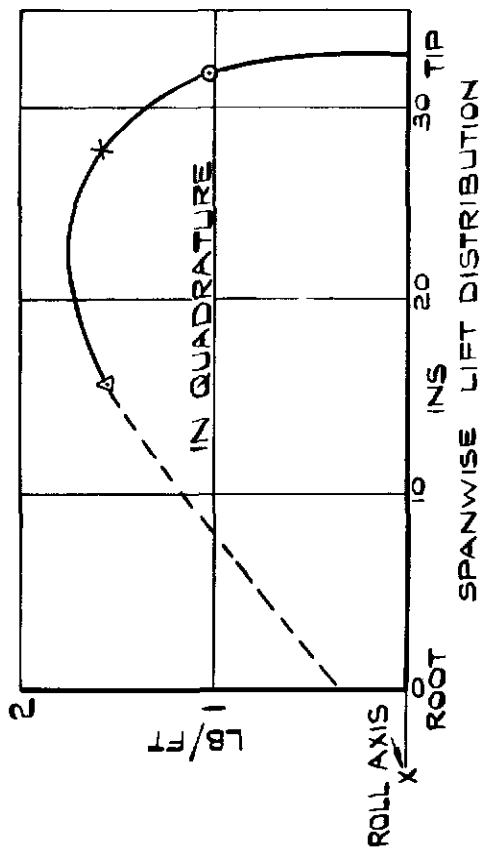
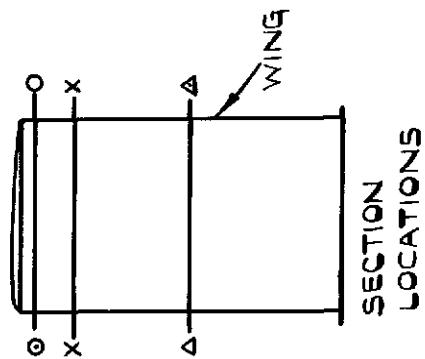
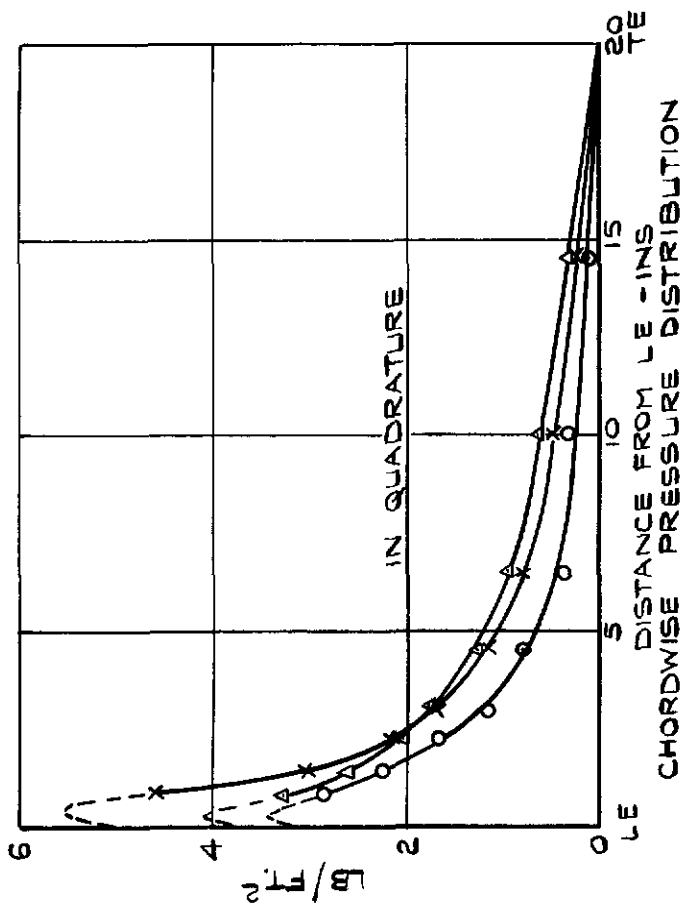


FIG. 12. SPANWISE DISTRIBUTION OF ROLLING MOMENT ABOUT WING ROOT - WING PITCH.



VELOCITY = 240 FT/SEC
 ROLL ANGLE = ±102 DEGREES
 FREQUENCY = 630 CYCLES/SEC.

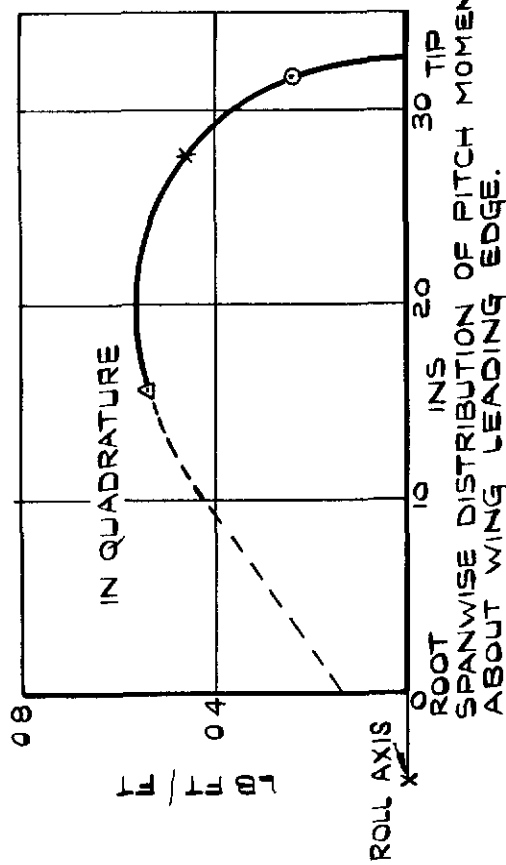
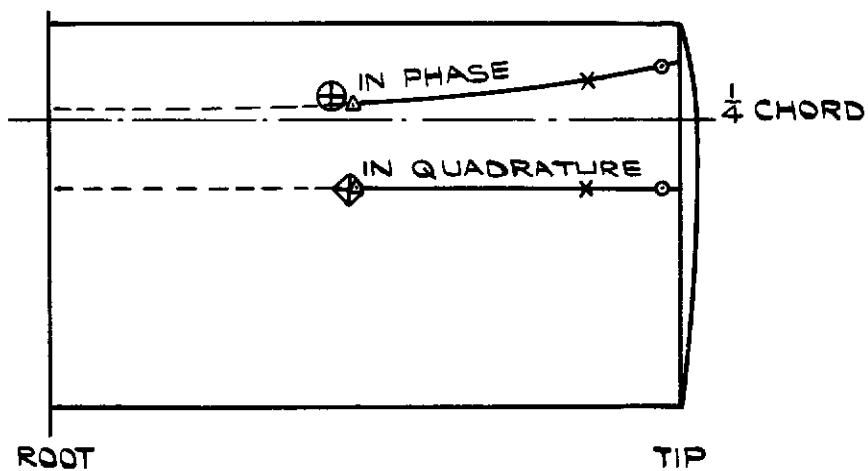
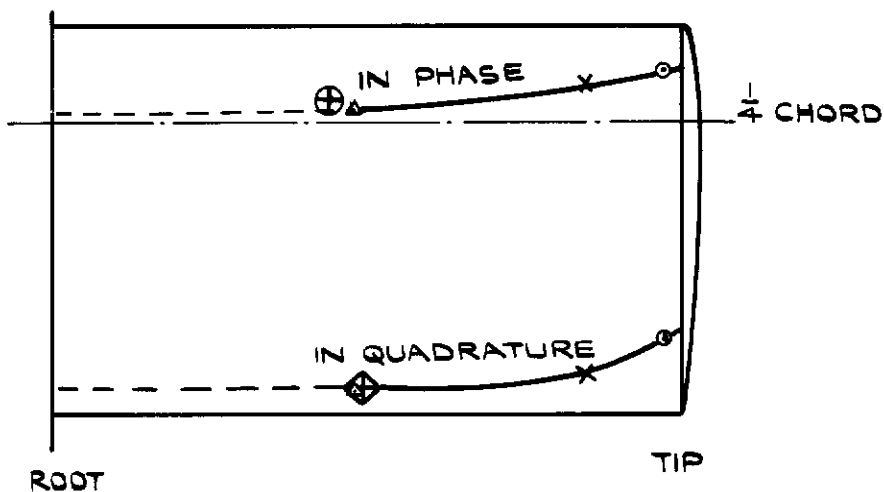


FIG. 13. PRESSURE, LIFT, PITCH MOMENT AND ROLL MOMENT DISTRIBUTIONS - WING ROLL.

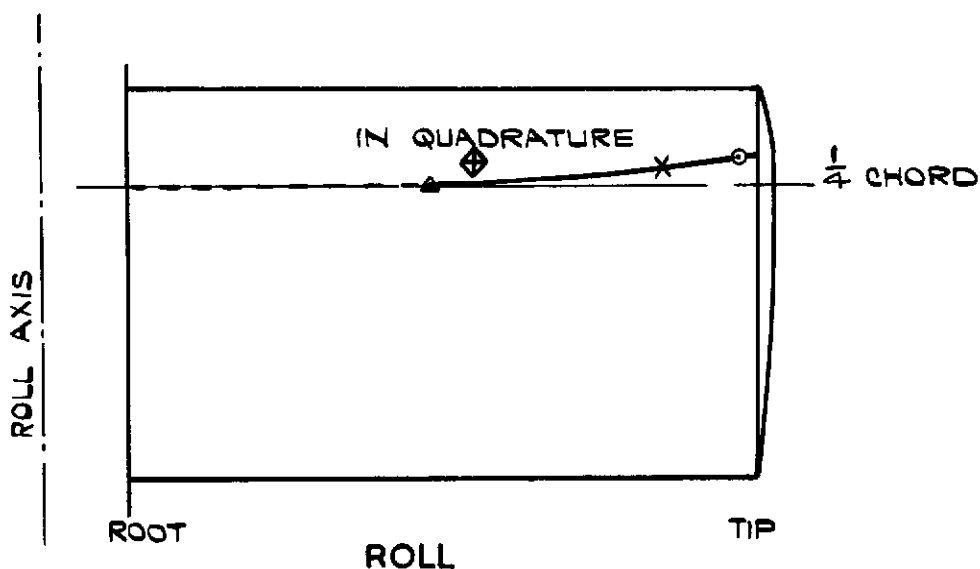
FIG.14.



PITCH ABOUT LEADING EDGE.



PITCH ABOUT TRAILING EDGE.



CENTRES OF PRESSURE FOR WHOLE WING SHOWN THUS $\left\{ \begin{array}{l} \text{IN PHASE } \oplus \\ \text{IN QUADRATURE } \diamond \end{array} \right.$

FIG.14.SPANWISE VARIATION OF AERODYNAMIC AXIS POSITIONS.

Crown copyright reserved

Published by
HER MAJESTY'S STATIONERY OFFICE

To be purchased from
York House, Kingsway, London W C 2
423 Oxford Street, London W 1
P O Box 569, London S E 1
13A Castle Street, Edinburgh 2
109 St Mary Street, Cardiff
39 King Street, Manchester 2
Tower Lane, Bristol 1
2 Edmund Street, Birmingham 3
80 Chichester Street, Belfast
or through any bookseller

PRINTED IN GREAT BRITAIN